Mobility Gradient in Surface Region of Monodisperse Polystyrene Films

Daisuke Kawaguchi, Keiji Tanaka, and Tisato Kajiyama*

Department of Applied Chemistry, Faculty of Engineering, Kyushu University, Fukuoka 812-8581, Japan

Atsushi Takahara

Institute for Fundamental Research of Organic Chemistry, Kyushu University, Fukuoka 812-8581, Japan

Seiji Tasaki

Research Reactor Institute, Kyoto University, Osaka 590-0494, Japan

Received September 11, 2002; Revised Manuscript Received December 18, 2002

ABSTRACT: Surface mobility in polystyrene (PS) films was studied using (PS/deuterated PS) bilayer films, which were prepared by attaching original two surfaces together. Time evolution of the bilayer interface at various temperatures was examined by dynamic secondary ion mass spectroscopy in conjunction with neutron reflectivity. When the bilayer was annealed at a temperature above bulk glass transition temperature, T_g^b, the interfacial thickening was well expressed by the context of Fickian diffusion. On the other hand, in the case of an annealing temperature above surface glass transition temperature, T_g^s, and below T_g^b, the interface monotonically thickened with the time at first and then turned to be independent. This means that chains went across the "*mobile*" interface and then reached the "*dead*" bulk region in which the diffusivity should be frozen. Hence, it was claimed that chains could diffuse discernibly in the surface region even at a temperature lower than the T_g^b. On the basis of temperature and molecular weight dependences of quasi-equilibrium interfacial thickness after a sufficiently long time, a possible model of mobility gradient in the surface region was proposed.

Introduction

Polymer surfaces play an important role in the field of polymer technology through the processes of wetting, friction, and adhesion.[1] In addition, they have been now recognized as crucial factors to construct highly and intriguing functionalized materials such as permselective membranes, biomaterials, etc.[2] Hence, it is of importance to understand precisely how surfaces differ from bulks, structurally and dynamically.

So far, surface mobility and dynamics have been widely explored by many research groups with the advent of modern spectroscopic and microscopic methods. Their conclusions seem to be based on that surface mobility is much enhanced in comparison with the corresponding bulk one,[3−15] although contradictory arguments have been going on.[16−21] We, combining temperature and angular-dependent X-ray photoelectron spectroscopy, studied the surface reorganization process in poly(styrene-*block*-methyl methacrylate) diblock copolymer films being in a nonequilibrium state with annealing.[22] A characteristic temperature, at which the surface chemical composition started to change, was much lower than the bulk glass transition temperature, T_g^b, and the depression became remarkably closer to the outermost surface. Since such a composition change can be attained only by molecular motion with a relatively large scale, this result implies that there is a mobility gradient in the surface region. Jean et al. have used Doppler broadening of energy spectra of annihilation radiation coupled with a slow positron beam to investigate T_g near the surface of polystyrene (PS).[5] They made a great success that T_g in the surface thin layer drastically decreased and its value was strongly dependent on the distance from the outermost surface. Also, surface dynamics can be examined by probing surface relaxation in rubbed films. Liu et al. first conducted this technique and pursued surface relaxation in PS films by near-edge X-ray absorption fine structure (NEXAFS).[23] Since the NEXAFS dichroic ratio did not completely recover to zero below the T_g^b, they concluded that molecular motion at the PS surface was not activated in comparison with that in the bulk, although the dichroic ratio at the surface started to decrease around 333 K, being much lower than the T_g^b. Schwab and co-workers made a similar experiment but with optical birefringence.[8] Then, they clearly showed that chains closer to the outermost surface relaxed much faster than bulk ones. This was well advocated by a work of Wallace et al. using NEXAFS.[13] Besides, Kerle et al. directly observed by atomic force microcopy that artificially rough PS surfaces started to flatten out even at a temperature below the T_g^b.[12] In contrast, Pu et al. have systematically worked on surface dynamics using shear modulation force microscopy and dynamic secondary ion mass spectroscopy and argued that there is no evidence of any peculiarities for surface mobility and dynamics.[20]

Glass transition and dynamics in thin films have been also attracted much attention due to scientific interests for a finite size effect on T_g as well as the importance of coating technologies. In particular, T_g in the thin films has been examined using ellipsometry,[24,25] Brillouin light scattering,[26] and X-ray reflectivity.[27,28] Keddie et al. found that T_g started to decrease as the film became

* To whom correspondence should be addressed: FAX +81-92-651-5606; Tel +81-92-642-3560; e-mail kajiyama@cstf.kyushu-u.ac.jp.

10.1021/ma025667f CCC: $25.00
Published on Web 01/29/2003

Table 1. Characterizations of Monodisperse Polystyrenes (hPS) and Deuterated Polystyrenes (dPS) Used in This Study

sample	M_n	M_w/M_n	T_g^b/K	T_g^s/K[d]
hPS-190K[a]	190K	1.09	386	335
dPS-185K[b]	185K	1.02	381	335
hPS-116K[b]	116K	1.04	384	320
dPS-111K[b]	111K	1.07	380	320
hPS-74K[b]	74K	1.04	382	310
dPS-76K[b]	76K	1.04	381	310
hPS-53K[c]	53K	1.04	378	292
dPS-50K[b]	50K	1.04	375	292
hPS-29K[c]	29K	1.09	376	264
dPS-29K[b]	29K	1.03	373	264

[a] Purchased from TOSOH Co. Ltd. [b] Purchased from Polymer Source Inc. [c] Synthesized by using living anionic polymerization. [d] Satomi et al. *Macromolecules* **2001**, *34*, 8761.

thinner than approximately 50 nm.[25] They took a notion of a liquidlike layer at the surface to rationalize what they observed. This model has been widely supported by following many different experiments.[29−31] Later, Kawana and Jones indicated a possibility that the thickness of such a liquidlike layer was of the order of 10 nm.[32] Independently, Kim et al. anticipated the depth-dependent T_g profile based on a continuous multilayer model.[33] Their model convincingly showed that surface glass transition temperature, T_g^s, was much lower than T_g^b and gradually approached the T_g^b with increasing distance from the surface. There have been several attempts to clarify the depth dependence of surface mobility. However, there seems to be a lack of experimental evidence for it.

Judging from the aforementioned experiments, it is reasonable to infer that polymer chains existed at the surface can diffuse even at a temperature lower than the T_g^b as long as the temperature is higher than the T_g^s. Perpendicular diffusion in the surface region can be examined by using a bilayer film composed of two different components in which the two original surfaces stand face-to-face.[34−37] Following an annealing treatment, the bilayer interface is broadened on account of the chain interdiffusion. We previously reported the time evolution of interfacial thickness for the bilayer films composed of PS and deuterated PS (hPS/dPS) at a given temperature below T_g^b as a communication.[38] At that time, the number-average molecular weight, M_n, of each component was fixed to be small of 29K. To complete the set of experiments, the time evolution of interfacial thickness should be examined for different temperatures and M_n's because chain diffusion strongly depends on the both. For this study, the following three issues will be discussed: (1) To what extent is the thickness of surface mobile layer? (2) What is the relation of the surface mobile layer to the chain dimension? (3) Is there a mobility gradient in the surface region, or otherwise, is it a uniform mobile layer?

Experimental Section

Polymers used in this study were monodisperse PS (hPS) and deuterated PS (dPS), which were synthesized by a living anionic polymerization or purchased. The chemical structures at both chain ends were composed of a *sec*-butyl group and a repeating unit terminated by proton. Table 1 tabulates M_n, the molecular weight distribution, M_w/M_n, where M_w denotes weight-average molecular weight, and T_g^b of the polymers. M_n and M_w/M_n were measured by gel permeation chromatography (GPC) with PS standards. T_g^b of hPS and dPS was determined by differential scanning calorimetry (DSC). Also, T_g^s of hPS and dPS was interpolated on the basis of the molecular weight dependence of T_g^s for the hPS examined by scanning viscoelasticity microscopy.[3d]

Laminated (hPS/dPS) bilayer films were prepared by a floating method, which has been mentioned in detail elsewhere.[38] At first, the bottom dPS layer for the bilayer was coated from a toluene solution onto a silicon wafer by the spin-coating method. The thickness of this layer was approximately 300 nm. The top hPS film with the almost same thickness was independently coated onto a microscope slide glass by a similar manner. Both films were annealed at 393 K for at least 36 h in vacuo to remove the residual solvent and the strain imposed by the film preparation process. The perimeter of the hPS film was scored with a blade, and the film was successively floated off onto the surface of 2.7 wt % 1-hydro-2-fluoroammonium solution. Then, the hPS film was picked up onto the dPS film by attaching the dPS film from the air side, resulting in that the bilayer interface was built up by two original surfaces of the hPS and dPS films.

For interdiffusion experiment, the bilayers were annealed under nitrogen atmosphere at various temperatures. The oven temperature was set to be the middle between the T_g^s and the T_g^b or well above the T_g^b. Once the inside temperature of the oven reached a constant, the bilayers were stored in the oven. Then, the annealing time was started to count. After a given time, the bilayers were rapidly quenched by immersing them into liquid nitrogen. The temperature calibration was made using mercury thermometers, which can measure the first decimal point. The temperature accuracy was 0.5 K.

Annealing-induced interfacial evolution of the bilayers was examined by dynamic secondary ion mass spectroscopy (DSIMS) (SIMS 4000, Seiko Instruments Inc., Atomika Analysetechnik GmbH). To gain access to a stable sputtering during the measurement, the buffer dPS layer was laminated onto the (hPS/dPS) bilayer by the floating technique. The thickness of the buffer dPS layer was approximately 200 nm. The incident beam of oxygen ions with 4 keV and ca. 30 nA was focused onto a 200 μm × 200 μm area of the specimen surface. The incident angle was 45°. A gold layer of 20 nm thickness was sputter-coated on the bilayer surface to avoid a charging of the specimen during the DSIMS measurement.

Neutron reflectivity (NR) measurements were carried out using the multilayer interferometer for neutrons (C3-1-2, MINE) at the Institute for Solid State Physics, the University of Tokyo. The incident neutrons have a wavelength of 1.26 nm and a resolution of 3.5%. The reflectivity was calculated on the basis of the scattering length density profile along the depth direction by using Spreadsheet Environmental Reflectivity Fitting.[39] For the NR measurement, bilayers composed of top hPS and bottom dPS layers with the thickness of approximately 50 nm were used to facilitate later fitting procedure. In this case, the upper hPS layer was not annealed above T_g^b before the lamination, since the film was too thin to float off onto the liquid surface after the annealing. Also, it was preconfirmed that this thickness did not affect the interdiffusion experiments.

Results and Discussion

Figure 1 shows a typical DSIMS profile of proton, H^+, deuterium, D^+, and carbon ions, C^+, for the (hPS/dPS) bilayer. For the first few minutes, the outrermost gold layer was etched, resulting in that secondary ions from the polymers were not clearly detected. After the gold layer, the C^+ intensity started to increase and then remained an almost constant through the bilayer. Hence, it can be judged that the steady-state etching proceeded during the measurement. While the D^+ intensity was relatively stronger than the H^+ one in the buffer dPS layer, the intensity relation became opposite in the hPS layer. Then, the relation of D^+ to H^+ intensity was again recovered when the etching reached the bottom dPS layer. Postulating that a constant etching was attained through the bilayer, the abscissa of etching

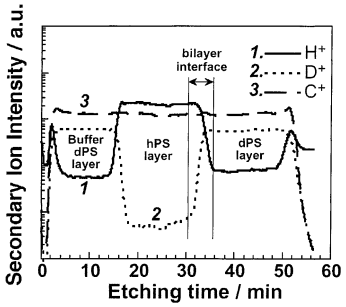

Figure 1. Typical DSIMS profile of proton, H^+, deuterium, D^+, and carbon, C^+, ions for the (hPS/dPS) bilayer. For stable experiments, gold and buffer dPS layers were mounted on the bilayer. The interfacial broadening of the bilayer was discussed on the basis of D^+ intensity change.

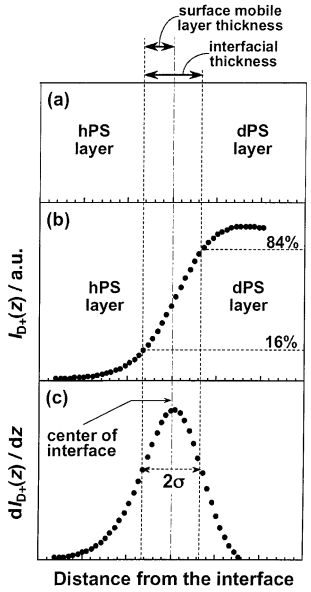

Figure 2. Our definition of the interfacial thickness: (a) cartoon showing bilayer configuration composed of hPS and dPS; (b) deuterium ion intensity profile, $I_{D+}(z)$, through the interface; (c) derivative of $I_{D+}(z)$ by the distance from the center of the interface. See text for details.

time can be simply converted to the depth from the surface. The etching rate was preexamined using the dPS film with a known thickness. We are interested in the thickness of the (hPS/dPS) bilayer interface marked in Figure 1.

A measured concentration profile by DSIMS is generally broadened from an ideal one owing to an atomic mixing effect. The broadening of the obtained profile was quantified by the instrument function, Δz_g, corresponding to the depth resolution. Figure 2 shows our definition of the interfacial thickness: (a) the cartoon showing the bilayer configuration, (b) the deuterium ion intensity profile $I_{D+}(z)$ through the interface, and (c) the derivative of $I_{D+}(z)$ by the distance from the center of the interface. Assuming that the $dI_{D+}(z)/dz$ can be expressed by Gaussian function as shown in Figure 2c, the Δz_i (i = g or m) is defined as twice the standard deviation of Gaussian function, corresponding to the depth range where I_{D+} rises from 16% to 84% of the maximum value.[34] The Δz_m denotes the measured apparent width of the bilayer interface. Using (hPS-190K/dPS-185K) bilayer film without annealing treatment, the Δz_g was estimated to be 7.4 nm. Hereafter, the number following each polymer species denotes its M_n. Since the interdiffusion at this bilayer interface cannot take place due

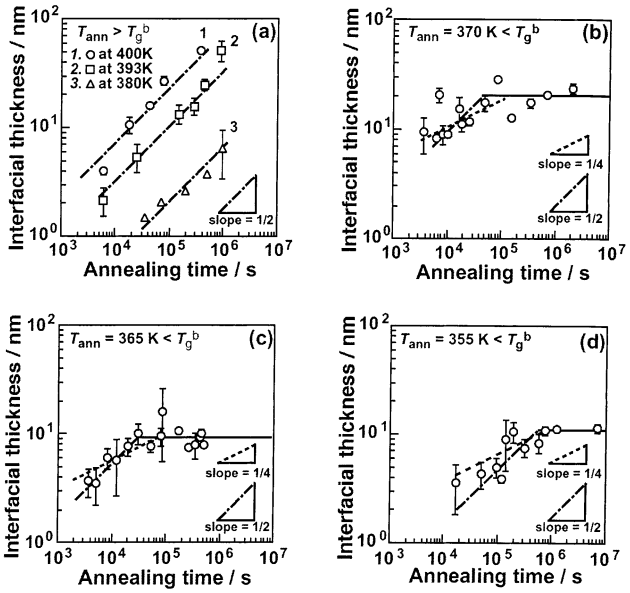

Figure 3. Double-logarithmic plots of the relation between interfacial thickness and annealing time for (hPS/dPS) bilayer annealed at various temperatures: (a) 400, 393, and 380 K above both T_g^b and T_g^s; (b) 370 K below T_g^b and above T_g^s; (c) 365 K below T_g^b and above T_g^s; (d) 355 K below T_g^b and above T_g^s. The broken and dotted lines are drawn in the context of Fickian and segmental diffusions, respectively.

to the T_g^s of 335 K being much higher than room temperature,[3c,d] the measured interfacial width can be regarded as the Δz_g. Then, the real interfacial thickness Δz is given in terms of the Δz_m and the Δz_g.[34]

$$\Delta z = (\Delta z_m^2 - \Delta z_g^2)^{1/2} \quad (1)$$

Diffusion behavior of polymers strongly depends on temperature and molecular weight. First, it was examined whether the interfacial thickness increased even at a temperature below the T_g^b. Parts a−d of Figure 3 show the time evolution of interfacial thickness for the (hPS-29K/dPS-29K) bilayer as a function of temperature. Since the hPS film with M_n of 29K was very fragile, it was almost impossible to construct the well-defined bilayer film with a large area. Hence, NR with a superior depth resolution to DSIMS could not be applied to the (hPS-29K/dPS-29K) bilayers. In the case of the annealing at 400, 393, and 380 K being above the T_g^b of 376 K, the interfacial thickness proportionally increased to a half power of the annealing time, t. This is in good accordance with the context of Fickian diffusion. On the contrary, a unique interfacial evolution was observed at 370 K being in between the T_g^s and the T_g^b. At first, the bilayer interface monotonically thickened with increasing t, although the exponent of t could be hardly determined because of the data scattering. When t proceeded to 10^5 s, however, the interfacial thickness remained the constant of 20 ± 5.6 nm. Here, it should be reminded that the bilayer interface was prepared by attaching two original surfaces of hPS and dPS together. Thus, the data mean that chains went across the "*mobile*" interface and then reached the "*dead*" bulk region in terms of diffusivity. In other words, half of the constant interfacial thickness evolved after a sufficiently long time would correspond to the surface layer, in which the mobility is enhanced in comparison with the internal bulk phase. We here define this layer as the "*surface mobile layer*", as shown in Figure 2a. Deferring

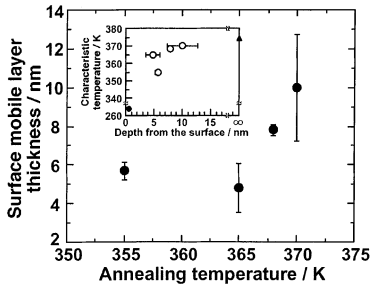

Figure 4. Annealing temperature dependence of surface mobile layer thickness. The inset was basically drawn replacing the abscissa and the ordinate of the main panel with each other, showing the relation between depth from the surface and characteristic temperature. The characteristic temperature corresponds to a temperature at which a large-scale motion can start to take place. The filled circle and triangle in the inset denote T_g^s and T_g^b, respectively.

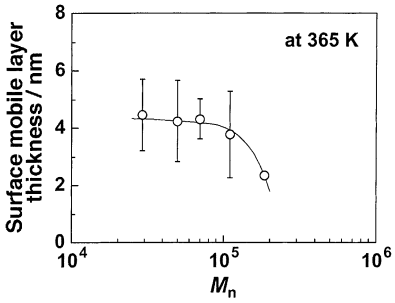

Figure 5. Molecular weight dependence of surface layer thickness at 365 K.

what the assumption of this notion is, the annealing temperature dependence of such a surface mobile layer is discussed. At 370 K, the thickness of the surface mobile layer was 10 ± 2.8 nm. It should be of interest to compare the thickness with the chain dimension. Twice the radius of gyration, $2R_g$, of an unperturbed PS-29K is calculated to be 9.3 nm by $2(Nb^2/6)^{1/2}$, where N and b are the degree of polymerization and the Kuhn's statistical segment length, respectively. This value is comparable to the surface layer thickness. Hence, it seems most likely that the quasi-equilibrium interfacial thickness was attained by center-of-mass diffusion such as Fickian. At 365 and 355 K, the interfacial thicknesses similarly increased with t at first and then turned to be invariant with respect to the annealing time, as shown in the parts c and d of Figure 3. The evolved interfacial thickness at 365 and 355 K were 9.6 ± 2.5 and 11.4 ± 0.9 nm, respectively. Half of these values, namely surface mobile layer thicknesses, are much smaller than the unperturbed chain dimension, implying that segmental diffusion dominates the interfacial broadening of the (hPS/dPS) bilayers at 365 and 355 K rather than center-of-mass diffusion.

DSIMS measurement revealed the relation between annealing temperature and quasi-equilibrium interfacial thickness for the (hPS-29K/dPS-29K) bilayer films. This gives rise to the discussion about mobility gradient in the surface region. The main panel of Figure 4 shows the annealing temperature variance with surface mobile layer thickness, which is drawn from Figure 3. This figure indicates the surface depth, in which molecular motion with a relatively large scale can be attained, at a given temperature. Replacing the abscissa and the ordinate by each other, the inset figure is obtained. In this case, the ordinate can be regarded as characteristic temperature at which the large-scale motion starts to take place. That is, the inset implies the depth dependence of characteristic temperature. For a comparison, the T_g^s of 264 K estimated by scanning force microscopy[3c] and the T_g^b of 376 K were also plotted at the depths of 0.5 nm and infinity, respectively, although the aforementioned characteristic temperature was not necessarily the same as glass transition temperature. Here, we should consider an undesirable and unavoidable situation of our experiment. Since the bilayer interface used to be two surfaces, the interfacial mobility can be directly regarded as the surface mobility right after the annealing is started. Then, the enhanced mobility at the interface, arisen originally from the surfaces, gradually disappears with proceeding interdiffusion. However, such a vigorous diffusivity at the interface can in part persist unless the annealing is made at a temperature above the T_g^b. Therefore, the notion of the surface mobile layer is still effective as long as the annealing temperature is below the T_g^b, provided that the absolute value of the surface layer thickness is supposed to be underestimated.[40] In any event, it can be qualitatively claimed from the inset of Figure 4 that there is a mobility gradient in the surface region of the hPS and dPS films and that surface chains and/or segments can diffuse even at a temperature below the T_g^b. This is in good agreement with our previous conclusion that the surface of the hPS-29K film is in a rubbery state, unlike the bulk region, even at room temperature.[3c,d] In a sense of surface dynamics with a relatively large scale motion, our conclusion made after Figure 4 is also consistent with many different experiments.[8,12,13]

So far, we have accounted for the active surface mobility by preferential segregation of chain end groups and reduced cooperativity for the segmental motion.[3] The depth range in which chain ends were enriched was on the order of a few nanometers.[41,42] Since the chain ends have a larger freedom than the main chain part, an excess free volume is induced in such depth region, resulting in enhanced mobility. Besides, the characteristic length scale of cooperativity for the segmental motion has been elucidated to be a few nanometers,[43,44] meaning that dynamics becomes faster within a depth shallower than this length scale. Nevertheless, the surface mobile layer became thicker beyond a few nanometers with increasing temperature, as shown in the main panel of Figure 4. For the moment, it can be hardly rationalized how such enhanced mobility propagates from the outermost surface to a deeper region. This is an interesting and challenging issue which should be addressed in the near future to understand the origin of the peculiar surface dynamics.

Figure 5 shows the molecular weight dependence of surface mobile layer thickness at 365 K. This temperature was well below T_g^b for the all samples. Once it was confirmed that each bilayer interface was no longer evolved, the annealing treatment for the (hPS/dPS) bilayers was stopped. The surface layer thickness was apparently insensitive to M_n up to 110K and then started to decrease with increasing M_n. Since the thickness was not scaled by $M_n^{1/2}$, it is clear that the thickness of the surface mobile layer is independent of the chain dimension; the thickness was not apparently related to the T_g difference between surface and bulk. Then, a question should be addressed is why such a molecular weight dependence appeared in Figure 5. We again recall the chain end effect as the responsible factor on the enhanced surface mobility. Figure 6 illustrates

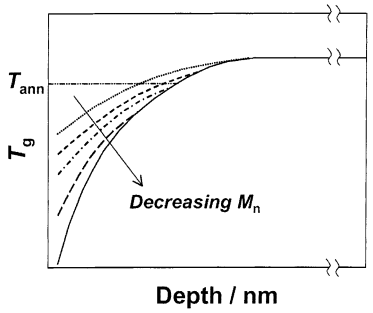

Figure 6. A possible model for depth dependence of T_g as a function of M_n, showing the mobility gradient in the surface region. Within the depth region in which chain ends are segregated, the mobility gradient should be strongly dependent on M_n. This would be not the case far beyond the segregated surface layer of chain ends.

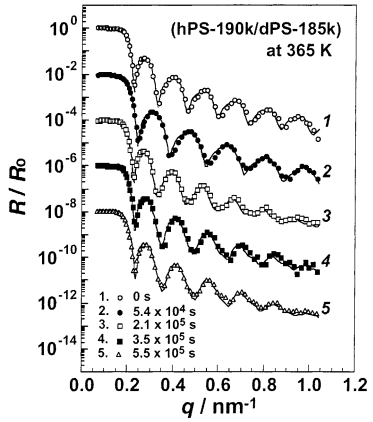

Figure 7. Neutron reflectivity curves of the as-prepared (hPS-190K/dPS-185K) bilayer and annealed ones at 365 K for various times. Experimental data sets are shown by symbols, and the best-fit curves calculated model scattering density profiles shown in Figure 8 are expressed by solid lines. The curves are vertically offset for clarity.

a possible cartoon of mobility gradients in the surface region, which was drawn by expanding the inset of Figure 4. At the depth range of a few nanometers from the surface, T_g should be strongly dependent on M_n because the concentration of segregated chain ends is connected to M_n.[3c,d] Once the depth goes far beyond the segregation layer of chain ends, there is no reason why the mobility gradient in the surface region depends on M_n.[45] This might be what was observed in Figure 5.

Finally, we come to the interdiffusion experiment by NR, which is a supplemental technique of DSIMS. Bilayers composed of hPS and dPS with the higher M_n of 190K were used. In this case, since the change in interfacial thickness upon annealing is predicted to be quite small due to its higher M_n, NR with the depth resolution better than 1 nm will be a powerful and promising technique.[46−50] The thickness of each component layer employed was approximately 50 nm, which was nearly equal to $4R_g$, so that the following fitting procedure of the experimental reflectivity became easier by virtue of the appearance of Kiessig fringe. To other groups[25,26,49,51] as well as ourselves,[52] substrate and chain confinement effects on surface mobility began to be remarkable as the thickness felt short of approximately $3R_g$. Thus, any thinning effects on surface mobility would be negligible in this thickness range. Actually, this will be later confirmed. Figure 7 shows the NR curves for the (hPS-190K/dPS-185K) bilayer film annealed at 365 K for various times. The solid lines

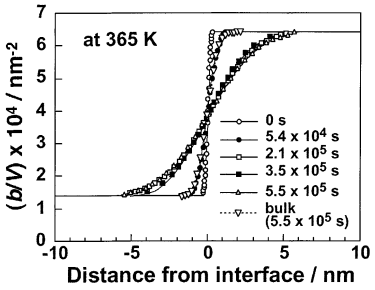

Figure 8. Scattering length density profiles at the as-prepared (hPS-190K/dPS-185K) interface and annealed ones at 365 K for various times.

denote the best-fit calculated reflectivity to the experimental one based on model scattering length density (b/V) profiles normal to the surface shown in Figure 8. Since the calculated curves were in good agreement with the experimental data, it can be claimed that the model (b/V) profiles correspond well to the composition profiles in the bilayer film along the direction perpendicular to the surface. For the hPS and the dPS, the (b/V) values of 1.41×10^{-4} and 6.46×10^{-4} nm^{-2} were used, respectively. When the annealing time increased, the bilayer interface broadened out, resulting in gradual loss of the sharpness for higher order fringes on the reflectivity curves. For quantitative analysis, the interfacial thickness can be defined as the depth range where the volume fraction of hPS-190K rises from 16% to 84% in the same manner as the DSIMS profile. The interfacial thickness monotonically increased with the annealing and then reached a constant value of 4.7 nm at 5.5×10^5 s. This interfacial evolution behavior was quite similar to parts b−d of Figure 3 by DSIMS. Also, half of the quasi-equilibrium interfacial thickness by NR was 2.4 nm and was equal to the one by DSIMS. Thus, it is apparent that our conclusion was, of course, independent of which experimental technique was used. Comparing the thicknesses of the surface mobile layer obtained by NR and DSIMS, it is also conceivable that any thinning effects on surface mobility were not crucial in the thickness range down to 50 nm. Using the bulk diffusion coefficient being under the same conditions, temperature, and M_n, after 5.5×10^5 s,[53] the interfacial broadening was predicted by open reverse triangles in Figure 8. This would help to see how mobile the surface layer is in comparison with the bulk.

Forrest and Dalnoki-Veress also studied the interfacial thickness of (hPS-115K/dPS-209K) bilayer based on NR measurements.[54] They observed the interfacial thicknesses of 0.9 and 0.6 nm after annealing at 363 and 322 K for the given time of 3 h, respectively. These values are much less than our results of 4.8 nm for the (hPS-190K/dPS-185K) bilayer annealed at 365 K. This may be because their annealing time of 3 h was much shorter than ours. Thus, it is plausible that their bilayer interface was still on the way to the quasi-equilibrium state.

Conclusions

The presence of a mobility gradient in the surface region of PS was confirmed on the basis of interdiffusion experiments using the (hPS/dPS) bilayers. The thickness of the (hPS/dPS) bilayer interface was definitely evolved with time even at a temperature below the T_g^b. This means that the surface mobility was much enhanced in comparison with the bulk. The thickness of

the surface mobile layer was of the order of nanometers, depending on the temperature and the molecular weight. In the surface layer, there is a gradient of chain and/or segmental mobility. Besides, the surface layer is not apparently related to the chain dimension.

Acknowledgment. We are most grateful for helpful discussions with Dr. Naoya Torikai and Dr. Masayasu Takeda. This was in part supported by a Grant-in-Aid for Scientific Research (A) (#13355034) from the Ministry of Education, Culture, Sports, Science, and Technology, Japan, and by Research Fellowships of the Japan Society for the Promotion of Science for Young Scientists. Also, this was partially supported by the Inter-Univ. Program for common use JAERI facility.

References and Notes

(1) Sanchez, I. C. *Physics of Polymer Surfaces and Interfaces*; Butterworth-Heinemann: Boston, 1992.
(2) Garbbasi, F.; Morra, M.; Occhiello, E. *Polymer Surfaces from Physics to Technology*; Wiley: New York, 1994.
(3) Kajiyama, T.; Tanaka, K.; Ohki, I.; Ge, S.-R.; Yoon, J.-S.; Takahara, A. *Macromoelcules* **1994**, *27*, 7932. (b) Kajiyama, T.; Tanaka, K.; Takahara, A. *Macromolecules* **1997**, *30*, 280. (c) Tanaka, K.; Takahara, A.; Kajiyama, T. *Macromolecules* **2000**, *33*, 7588. (d) Satomi, N.; Tanaka, K.; Takahara, A.; Kajiyama, T.; Ishizone, T.; Nakahama, S. *Macromolecules* **2001**, *34*, 8761. (e) Tanaka, K.; Takahara, A.; Kajiyama, T.; Tasaki, S. *Macromolecules* **2002**, *35*, 4702.
(4) Meyers, G. F.; DeKoven, B. M.; Seitz, J. T. *Langmuir* **1992**, *8*, 2330.
(5) Jean, Y. C.; Zhang, R.; Cao, H.; Yuan, J. P.; Huang, C. M.; Nielsen, B.; Asoka-Kumar, P. *Phys. Rev. B* **1997**, *56*, R8459.
(6) Hammerschmidt, J. A.; Gladfelter, W. L.; Haugstad, G. *Macromolecules* **1999**, *32*, 3360.
(7) Rouse, J. H.; Twaddle, P. L.; Ferguson, G. S. *Macromolecules* **1999**, *32*, 1665.
(8) Schwab, A. D.; Agra, D. M. G.; Kim, J. H.; Kumar, S.; Dhinojwala, A. *Macromolecules* **2000**, *33*, 4903.
(9) Fryer, D. S.; Nealey, P. F.; de Pablo, J. J. *Macromolecules* **2000**, *33*, 6439.
(10) Zaporojtchenko, V.; Strunskus, T.; Erichsen, J.; Faupel, F. *Macromolecules* **2001**, *34*, 1125.
(11) Hyun, J.; Aspnes, D. E.; Cuomo, J. J. *Macromolecules* **2001**, *34*, 2395.
(12) Kerle, T.; Lin, Z.; Kim, H. C.; Russell, T. P. *Macromolecules* **2001**, *34*, 3484.
(13) Wallace, W. E.; Fischer, D. A.; Efimenko, K.; Wu, W. L.; Genzer, J. *Macromolecules* **2001**, *34*, 5081.
(14) Fischer, H. *Macromolecules* **2002**, *35*, 3592.
(15) Bliznyuk, V. N.; Assender, H. E.; Briggs, G. A. D. *Macromolecules* **2002**, *35*, 6613.
(16) Xie, L.; DeMaggio, G. B.; Frieze, W. E.; DeVries, J.; Gidley, D. W.; Hristov, H. A.; Yee, A. F. *Phys. Rev. Lett.* **1995**, *74*, 4947.
(17) Gracias, D. H.; Zhang, D.; Lianos, L.; Ibach, W.; Shen, Y. R.; Somorjai, G. A. *Chem. Phys.* **1999**, *245*, 277.
(18) Tsui, O. K. C.; Wang, X. P.; Ho, J. Y. L.; Ng, T. K.; Xiao, X. *Macromolecules* **2000**, *33*, 4198. (b) Tsui, O. K. C.; Zhang, H. F. *Macromolecules* **2001**, *34*, 9139.
(19) Hamdorf, M.; Johannsmann, D. *J. Chem. Phys.* **2000**, *112*, 4262.
(20) Ge, S.; Pu, Y.; Zhang, W.; Rafailovich, M.; Sokolov, J.; Buenviaje, C.; Buckmaster, R.; Overney, R. M. *Phys. Rev. Lett.* **2000**, *85*, 2340. (b) Pu, Y.; Ge, S.; Rafailovich, M.; Sokolov, J.; Duan, Y.; Pearce, E.; Zaitsev, V.; Schwarz, S. *Langmuir* **2001**, *17*, 5865. (c) Pu, Y.; Rafailovich, M. H.; Sokolov, J.; Gersappe, D.; Peterson, T.; Wu, W. L.; Schwarz, S. A. *Phys. Rev. Lett.* **2001**, *87*, 206101.
(21) Weber, R.; Zimmermann, K. M.; Tolan, M.; Stettner, J.; Press, W.; Seeck, O. H.; Erichsen, J.; Zaporojtchenko, V.; Strunskus, T.; Faupel, F. *Phys. Rev. E* **2001**, *64*, 061508.
(22) Kajiyama, T.; Tanaka, K.; Takahara, A. *Macromolecules* **1995**, *28*, 3482.
(23) Liu, Y.; Russell, T. P.; Samant, M. G.; Stöhr, J.; Brown, H. R.; Cossy-Favre, A.; Diaz, J. *Macromolecules* **1997**, *30*, 7768.
(24) Beaucage, G.; Composto, R.; Stein, R. S. *J. Polym. Sci., Polym. Phys. Ed.* **1993**, *31*, 319.
(25) Keddie, J. L.; Jones, R. A. L.; Cory, R. A. *Europhys. Lett.* **1994**, *27*, 59. (b) Keddie, J. L.; Jones, R. A. L. *Faraday Discuss.* **1994**, *98*, 219.
(26) Forrest, J. A.; Dalnoki-Veress, K.; Stevens, J. R.; Dutcher, J. R. *Phys. Rev. Lett.* **1996**, *77*, 2002. (b) Forrest, J. A.; Dalnoki-Veress, K.; Dutcher, J. R. *Phys. Rev. E* **1997**, *56*, 5705.
(27) Wallace, W. E.; van Zanten, J. H.; Wu, W. L. *Phys. Rev. E* **1995**, *52*, R3329.
(28) Fryer, D. S.; Peters, R. D.; Kim, E. J.; Tomaszewski, J. E.; de Pablo, J. J.; Nealey, P. F.; White, C. C.; Wu, W. L. *Macromolecules* **2001**, *34*, 5627.
(29) Tseng, K. C.; Turro, N. J.; Durning, C. J. *Phys. Rev. E* **2000**, *61*, 1800.
(30) Fukao, K.; Miyamoto, Y. *Phys. Rev. E* **2000**, *61*, 1743.
(31) Xie, F.; Zhang, H. F.; Lee, F. K.; Du, B.; Tsui, O. K. C.; Yokoe, Y.; Tanaka, K.; Takahara, A.; Kajiyama, T.; He, T. *Macromolecules* **2002**, *35*, 1491.
(32) Kawana, S.; Jones, R. A. L. *Phys. Rev. E* **2001**, *63*, 021501.
(33) Kim, J. H.; Jang, J.; Zin, W. C. *Langmuir* **2001**, *17*, 2703.
(34) Whitlow, S. J.; Wool, R. P. *Macromolecules* **1991**, *24*, 5926.
(35) Stamm, M.; Hüttenbach, S.; Reiter, G.; Springer, T. *Europhys. Lett.* **1991**, *14*, 451.
(36) Karim, A.; Felcher, G. P.; Russell, T. P. *Macromolecules* **1994**, *27*, 6973.
(37) Boiko, Y. M.; Prud'homme, R. E. *J. Polym. Sci., Part B: Polym. Phys.* **1998**, *36*, 567.
(38) Kawaguchi, D.; Tanaka, K.; Takahara, A.; Kajiyama, T. *Macromolecules* **2001**, *34*, 6164.
(39) Welp, K. A.; Co, C. C.; Wool, R. P. *J. Neutron Res.* **1999**, *8*, 37.
(40) Thus, we have been trying to examine lateral diffusion of polymer chains at the free surface for the moment. This will be reported in the near future.
(41) Zhao, W.; Zhao, X.; Rafailovich, M. H.; Sokolov, J.; Composto, R. J.; Smith, S. D.; Satkowski, M.; Russell, T. P.; Dozier, W. D.; Mansfield, T. *Macromolecules* **1993**, *26*, 561.
(42) Tanaka, K.; Kawaguchi, D.; Yokoe, Y. Kajiyama, T.; Takahara, A., submitted for publication.
(43) Ngai, K. L.; Rizos, A. K. *Mater. Res. Soc. Symp. Proc.* **1997**, *455*, 147.
(44) Ediger, M. D. *Annu. Rev. Phys. Chem.* **2000**, *51*, 99.
(45) However, of course, it took a longer time for the higher M_n component to reach a quasi-equilibrium thickness of the bilayer interface owing to a slow diffusion.
(46) Russell, T. P. *Mater. Sci. Rep.* **1990**, *5*, 171.
(47) Zhao, W.; Zhao, X.; Rafailovich, M. H.; Sokolov, J.; Mansfield, T.; Stein, R. S.; Composto, R. J.; Kramer, E. J.; Jones, R. A. L.; Sansone, M.; Nelson, M. *Physica B* **1991**, *173*, 43.
(48) Kunz, K.; Stamm, M. *Macromolecules* **1996**, *29*, 2548.
(49) Lin, E. K.; Kolb, R.; Satija, S. K.; Wu, W. L. *Macromolecules* **1999**, *32*, 3753.
(50) Bucknall, D. G.; Butler, S. A.; Higgins, J. S. *Macromolecules* **1999**, *32*, 5453.
(51) Kuhlmann, T.; Kraus, J.; Müller-Buschbaum, P.; Schubert, D. W.; Stamm, M. *J. Non-Cryst. Solids* **1998**, *235−237*, 457.
(52) Akabori, K.; Tanaka, K.; Takahara, A.; Kajiyama, T. Manuscript in preparation.
(53) Green, P. F.; Kramer, E. J. *Macromolecules* **1986**, *19*, 1108.
(54) Forrest, J. A.; Dalnoki-Veress, K. *J. Polym. Sci., Part B: Polym. Phys.* **2001**, *39*, 2664.

MA025667F